Red blood cells ageing markers: a multi-parametric analysis

Manon Bardyn[1], Benjamin Rappaz[2], Keyvan Jaferzadeh[3], David Crettaz[1], Jean-Daniel Tissot[1], Inkyu Moon[3], Gerardo Turcatti[2], Niels Lion[1], Michel Prudent[1]

[1]Blood Products Research Laboratory, Interregional Blood Transfusion SRC, Epalinges, Switzerland; [2]Swiss Federal Institute of Technology, Biomolecular Screening Facility, School of Life Sciences, Lausanne, Switzerland; [3]Chosun University, School of Computer Engineering, Dong-Gu, Gwangju, South Korea

Background. Red blood cells collected in citrate-phosphate-dextrose can be stored for up to 42 days at 4 °C in saline-adenine-glucose-mannitol additive solution. During this controlled, but nevertheless artificial, *ex vivo* ageing, red blood cells accumulate lesions that can be reversible or irreversible upon transfusion. The aim of the present study is to follow several parameters reflecting cell metabolism, antioxidant defences, morphology and membrane dynamics during storage.

Materials and methods. Five erythrocyte concentrates were followed weekly during 71 days. Extracellular glucose and lactate concentrations, total antioxidant power, as well as reduced and oxidised intracellular glutathione levels were quantified. Microvesiculation, percentage of haemolysis and haematologic parameters were also evaluated. Finally, morphological changes and membrane fluctuations were recorded using label-free digital holographic microscopy.

Results. The antioxidant power as well as the intracellular glutathione concentration first increased, reaching maximal values after one and two weeks, respectively. Irreversible morphological lesions appeared during week 5, where discocytes began to transform into transient echinocytes and finally spherocytes. At the same time, the microvesiculation and haemolysis started to rise exponentially. After six weeks (expiration date), intracellular glutathione was reduced by 25%, reflecting increasing oxidative stress. The membrane fluctuations showed decreased amplitudes during shape transition from discocytes to spherocytes.

Discussion. Various types of lesions accumulated at different chemical and cellular levels during storage, which could impact their *in vivo* recovery after transfusion. A marked effect was observed after four weeks of storage, which corroborates recent clinical data. The prolonged follow-up period allowed the capture of deep storage lesions. Interestingly, and as previously described, the severity of the changes differed among donors.

Keywords: red blood cell, storage lesion, membrane fluctuation, digital holographic microscopy, antioxidant.

Introduction

During storage, red blood cells (RBCs) accumulate metabolic, oxidative and physiological lesions[1-4] that can be reversible or irreversible following transfusion[5]. Several studies assessed the adverse effects of transfusing long-term stored RBCs in humans and dogs[6-8]. Recently, Goel *et al.* demonstrated in a retrospective study that transfusion of RBCs of more than 35 days was associated with an increased length of stay in hospital, morbidity and mortality, especially for high-risk patients[9]. However, recent randomised trials, such as the Age of Blood Evaluation (ABLE)[10], the Red Cell Storage Duration study (RECESS)[11], and the Informing Fresh versus Old Red Cell Management (INFORM) trial[12] suggested that patients transfused with short- or long-term stored RBCs have similar clinical outcomes[13].

Storage at 4 °C not only prevents bacterial expansion, it also slows down RBC metabolism, thus limiting consumption of nutrients and accumulation of waste products[14,15]. For example, inhibition of the glycolytic enzyme phosphofructokinase at low temperature and low pH (when extracellular lactate level builds up)[16] results in rapid depletion of the oxygen-haemoglobin (Hb) affinity regulator 2,3-diphosphoglycerate (DPG)[17]. The membrane Na^+/K^+ pumps are also known to be inactivated at 4 °C, leading to loss of potassium and accumulation of intracellular sodium[18]. In a recent study, Paglia *et al.* proposed 8 extracellular compounds as biomarkers to describe the different metabolic phases during storage[19].

The RBCs packed in gas permeable blood bags are continuously exposed to oxygen. Consequently, when oxidative stress exceeds antioxidant defence,

oxidative injuries such as proteins oxidation and lipids peroxidation accumulate[20-26]. After four weeks of storage, it was hypothesised that the proteasome becomes unable to degrade accumulating cross-linked oxidised proteins which bind to the intracellular side of the membrane[3,15,21,22,27-29]. RBC metabolism is also impacted by oxidative stress. For example, oxidation was shown to modulate enzymatic activity of glyceraldehyde 3-phosphate dehydrogenase, thus re-routing glucose oxidation through the glycolysis or pentose phosphate pathway (PPP)[24,30]. Accumulation of cytosolic peroxiredoxin-2 at the inner cell membrane was proposed as a marker of oxidative stress in RBCs[31].

To eliminate altered proteins, lipids and other deleterious compounds, stored RBCs release phospholipids-rich, CD47-positive microvesicles (MVs)[28]. Among other proteins, extensively oxidised Hb at key functional residues was found in MVs during storage[32]. MV accumulation in the blood bags[33] has a haemostatic effect in transfusion recipients[34,35]. In addition, membrane loss by microvesiculation is an irreversible process during which biconcave RBCs progressively become echinocytes and finally spherocytes[36,37]. High membrane surface-to-volume ratio, as well as dynamic adenosine triphosphate (ATP)-dependent membrane-cytoskeleton remodelling, which are both decreased during storage, give their deformability to the RBCs allowing them to pass through small capillaries and deliver oxygen to peripheral organs/tissues[38-40]. RBCs that are poorly deformable and/or express senescent markers, such as increased externalised phosphatidylserine or decreased CD47 levels, are retained by the macrophages in transfusion recipient spleen and removed from circulation[41,42].

Ultimately, RBCs that are too extensively damaged lyse in the blood bag, releasing their cytosolic content[43]. Haemolysis biomarkers were recently discovered by proteomics analysis of erythrocyte concentrate (EC) supernatant[44]. Transfusion of long-term stored RBCs exhibiting a high percentage of haemolysis leads to an increase of the level of non-transferrin bound iron in the circulation of the patient[45]. In addition, cell-free Hb accumulates in the spleen, the kidney and/or the liver of the transfusion recipient[46-48]. This might induce transfusion-related complications such as increased inflammation and predisposition to infections[49,50].

Since morphological damage is related to biochemical lesions, our study aims at better characterising and quantifying storage lesions by looking at multiple ageing hallmarks all together. Therefore, 5 different ECs were followed during 71 days. Some metabolic parameters such as glucose consumption and extracellular lactate accumulation were quantified. Antioxidant power (AOP) was determined *via* the electrochemical pseudo-titration of water-soluble antioxidants[51,52] in the ECs as well as the measurement of the intracellular glutathione. Percentage of haemolysis and degree of microvesiculation were also assessed. Finally, digital holographic microscopy (DHM) was used to follow the changes of RBC morphology and the levels of dynamic cell membrane fluctuations (CMF), a parameter related to cell health state[53].

Material and methods

Preparation of the erythrocyte concentrates

The 5 ECs came from healthy donors (2 women and 3 men) who donated whole blood (refer to Online Supplementary Content). The products were prepared at the blood center of the Interregional Blood Transfusion SRC (Epalinges, Switzerland) as follows: 450±50 mL of whole blood were collected and mixed with 63 mL citrate-phosphate-dextrose (CPD) anticoagulant. The pouches were centrifuged to separate blood components, and a semi-automated pressure applied to distribute the blood fractions into sterile inter-connected blood bags (Fenwal, Lake Zurich, IL, USA). Finally, the erythrocytes were filtered to remove residual leukocytes and 100 mL of saline-adenine-glucose-mannitol (SAGM) additive solution were added. The 5 ECs (final volume of 275±75 mL and haematocrit [HCT] of 0.6±0.1 v/v) were stored at 4 °C and monitored during 71 days. Five mL of each sample were collected using a sampling site weekly during 71 days (twice during week 1, 2 and 4).

Intracellular glutathione

Quantification of intracellular reduced and oxidised glutathione (GSH and GSSG) was performed according to the protocol proposed by Giustarini *et al.*[54] with small modifications. This assay is based on GSH reaction with Ellman's reagent (5,5'-dithio-bis-[2-nitrobenzoic acid], [DTNB]) that produces TNB quantifiable by spectrophotometry at 412 nm. GSSG is recycled into GSH in the presence of glutathione reductase and reduced nicotinamide adenine dinucleotide phosphate (NADPH). Two mL of each EC were collected for the analysis, from which 750 µL were transferred into an empty tube for total glutathione quantification and 750 µL in a second tube containing 225 µL of the derivatising agent *N*-ethylmaleimide (NEM 300 mM, Sigma-Aldrich, Steinheim, Germany) for GSSG measurement. NEM is added to prevent oxidation of GSH into GSSG during the acid deproteinisation step. Samples were centrifuged at 10,000 *g*, 38 sec., 4 °C and supernatant was discarded. RBCs were then washed twice in 2 volumes of 1× phosphate buffered saline (PBS) (Laboratorium Dr. G. Bichsel, Interlaken, Switzerland). RBC pellet was resuspended in 1 volume of 1×PBS, and a Sysmex (KX-21N, Sysmex,

Horgen, Switzerland) measurement was performed to determine intracellular Hb concentration of each sample for normalisation. Two aliquots of 400 µL were transferred in new tubes, centrifuged as before, and supernatant was discarded. The samples were stored as dry pellets of RBCs at −80 °C until analysis. The rest of the analysis followed the procedure described in the protocol.

Haematologic, antioxidant power and microvesicle analyses

Approximately 500 µL samples were withdrawn from each ECs for haematologic, AOP and MVs analyses. Haematologic data were recorded with Sysmex automated haematology analyser. AOP of ECs was measured electrochemically using an Edelmeter potentiostat (EDEL-for-Life, Lausanne, Switzerland)[51]. A few microlitres (approximately 3 µL) of EC sample were loaded in a disposable screen-printed electrode chip and linear sweep voltammetry was recorded by the apparatus. AOP is reported in nW (1 nW being equivalent to the antioxidant activity of 1 µM of ascorbic acid in PBS). MVs were quantified by flow cytometry (FACScalibur flow cytometer with CellQuest pro software, BD Biosciences, Franklin Lakes, NJ, USA)[21,33]. Briefly, 5 µL of EC were mixed with 5 µL of FITC anti-human CD47 antibody (BD Biosciences, San Jose, CA, USA) and incubated 20 min. at room temperature under agitation. Before analysis, Trucount™ tubes (BD Biosciences, Franklin Lakes, NJ, USA) that contain a known amount of fluorescent beads enabling quantitation were filled with 400 µL of 0.9% NaCl (Laboratorium Dr. G. Bichsel) and 5 µL of labelled sample. The different populations in the sample were discriminated according to their size (forward scatter [FSC]), granularity (side scatter [SSC]) and fluorescence. Small (<1 µm) and CD47-positive events were considered as MVs.

Haemolysis, glucose and lactate quantitation in supernatants

Two and a half mL of EC samples were centrifuged at 2,000 *g*, 10 min. at 4 °C. The supernatants were collected for haemolysis measurement and stored at −80 °C for further analyses (extracellular glucose and lactate concentrations). RBCs were further processed for DHM analysis. The concentration of Hb in the supernatant for haemolysis quantitation was determined according to the Harboe method with the 3-point Allen correction[55]. Absorbance at 415, 380 and 450 nm was recorded with a spectrophotometer (NanoDrop 2000c, Thermo Fisher Scientific, Wilmington, Delaware, USA).

Extracellular concentrations of glucose and lactate were measured in supernatant samples using commercial colorimetric assays[56]. Glucose was quantified using a Biochain assay (kit Z5030025, BioChain, Newark, CA, USA) and lactate concentration with a BioVision assay (kit II, K627-100, BioVision, Milpitas, CA, USA).

Digital holographic microscopy experiments

Red blood cells were washed twice with 0.9% NaCl and spun down at 2,000 *g*, 10 min. at 4 °C. At the end of the washing step, RBCs were resuspended in 1 volume of NaCl 0.9%. Six hundred µL of each sample were taken into 1.5 mL tube, centrifuged as before, supernatants were discarded, and two volumes of HEPA 10 mM glucose (refer to Online Supplementary Content) were added on RBC pellets (Sysmex analysis was performed to determine the RBC concentration). RBCs were further diluted and seeded at a density of 75,000 cells in 100 µL per well (3 wells per EC) in a 96-well imaging plate (BD Falcon, Big Flats, NY, USA) coated with 0.1 mg/mL Poly-L-ornithine (Sigma-Aldrich). The plate was centrifuged at 140 *g*, 2 min. at room temperature to speed up the sedimentation process. During image acquisition, the plate was placed in a plate incubator set at 37 °C with high humidity and 5% CO_2.

The microscope used was a DHM® T1000 (Lyncée Tec SA, Lausanne, Switzerland) equipped with a motorised microscope stage (Märzhäuser Wetzlar GmbH & CO. KG, Wetzlar, Germany), an incubator system (LCI Live Cell Instrument, Seoul, South Korea), and Leica 20×/0.40 NA and 40×/0.75 NA objectives (Leica Microsystems GmbH, Wetzlar, Germany). Quantitative phase images (20× magnification, 4 images/well) and short movies (40× magnification, 10 sec., 20 images/sec.) of RBCs were acquired to analyse RBC morphology and membrane fluctuations, respectively. DHM is a non-invasive label-free interferometric microscopy technique which provides a quantitative measurement of the phase or optical path length (OPL, related to the morphology and Hb content of RBC)[57-60]. It is a 2-step process where a hologram consisting of a 2D interference pattern is first recorded on a digital camera and the quantitative OPL images are reconstructed numerically using a specific algorithm. The phase information in DHM is quantitatively related to the optical path difference (OPD), expressed in terms of cell biophysical parameters as described in the following equation:

$$OPD_{(x,y)} = d_{(x,y)} \times (n_{cell(x,y)} - n_m) \quad (1)$$

where $d_{(x,y)}$ is the cell thickness, $n_{cell(x,y)}$ the mean z-integrated intracellular refractive index (a property mainly linked to the protein concentration of cells[60]) at the (x,y) position and n_m the refractive index of the surrounding culture medium[61].

Concretely, as far as RBCs are concerned, the value of the intracellular refractive index results primarily from Hb concentration and is considered as constant. DHM system uses a low intensity laser as light source for specimen illumination and a digital camera to record the hologram. Here, the 684 nm laser source delivers roughly 200 μW/cm^2 at the specimen plane; that is some six orders of magnitude less than intensities typically associated with confocal fluorescence microscopy. With that amount of light, the exposure time is only 0.4 ms.

Red blood cell morphology analysis with digital holographic microscopy

Quantitative phase images were analysed in two ways. First, a population analysis (yielding a single output per image) was performed by automatic calculation of the standard deviation of the OPD distribution (SD-OPD) value during the reconstruction of the images, it has the advantage of being directly available without further analysis enabling high-throughput screening. The raw OPD images are thresholded with a fixed threshold value (slightly above background level to discard noisy pixels) to create the "cell mask", all the pixel OPD values that are within the mask are plotted in a histogram. The standard deviation of the distribution of OPD values is then calculated and averaged for the 4 images and used to quantify morphological changes occurring in RBCs.

Single-cell analysis was also performed using CellProfiler (Broad Institute, www.cellprofiler.org, 2.1.0 rev 0c7fb94) and CellProfiler Analyst (2.0 r11710)[62]. CellProfiler was first used to identify, segment and measure different parameters of the individual RBCs such as their area, size, intensity and granularity. CellProfiler Analyst (CPA) then uses these features during the supervised machine learning to classify RBCs in one of the four class that was defined: "stomatocytes", "discocytes", "echinocytes" and "spherocytes". An additional "errors" class was added to eliminate objects resulting from segmentation errors.

Red blood cell membrane fluctuations with digital holographic microscope

DHM phase images from each time-frame of the recorded movies were first registered using the StackReg ImageJ plugin[63] (to cancel the spatial displacement of RBCs) and then, using ImageJ[64], manually segmented into individual RBCs to measure membrane fluctuations at the single-RBC level. Membrane fluctuations amplitude were measured on individual cells according to Rappaz *et al.*[65] (refer to Online Supplementary Content). Fluctuations were computed for the four different shapes of RBC.

Data were analysed and plotted with Prism 7 software (GraphPad PRISM, La Jolla, CA, USA). Mean values for the 5 ECs were calculated with errors bars corresponding to the mean ± standard deviation. One-way ANOVA with Greenhouse-Geisser correction was performed to compare values at different storage time.

Results and discussion

Storage lesions appeared at different time points during the 71 days of follow up. Mean values for several ageing parameters at day 1, 29, 43 and 71 are presented in Table I.

Routine haematologic data

Haematologic parameters (Figure 1A) evolved similarly for all ECs at the exception of EC 5. Mean RBC corpuscular volume (MCV), initially of 89.5±4.3 fL, gained on average 5.1 fL at day 43 and 7.9 fL at day 71 (not including EC 5). Sizes of RBCs in the population became more heterogeneous during storage, as indicated by an increasing deviation of RBC distribution width (SD-RDW), a parameter providing information about the anisocytosis.

Extracellular glucose and lactate concentrations

The extracellular glucose (initial concentration of 481±33 mg/dL) was progressively consumed by the cells during storage, as indicated by the decline in concentration (Figure 1B, left). At day 52, a plateau value was reached at 180±29 mg/dL and did not decrease further. During the 71 days of storage, RBCs consumed on average 64% of the available glucose. In contrast, lactate, a glycolysis end product increased (Figure 1B, right). Mean lactate concentration increased from 6.6±1.0 mM at day 1 to reach a plateau at 36.5±3.3 mM at day 36 (5.6-fold increase).

Antioxidants

The global AOP in the 5 ECs increased during the first week of storage following blood collection (baseline mean AOP of 71.4±5.3 nW), reaching a maximal value (81.8±8.1 nW) at day 4. Then, the AOP decreased gradually until day 22 (65.5±6.3 nW) and remained stable until the end of follow up (Figure 1C, left). This behaviour, as recently demonstrated[52], suggests that RBCs are impacted by blood processing. This response can be passive (RBCs equilibrating with their new environment by releasing waste products and other molecules) or active. Uric acid is one of the antioxidant molecule excreted by the RBCs that is responsible for the increase of AOP[52]. This end-product of purine metabolism is present at concentrations close to its limit of water solubility in the blood plasma (120-450 μM) and is able to neutralise a broad range of ROS[66].

Table I - Main red blood cell parameters followed during storage.

	Day 1	Day 29	Day 43	Day 71
RBCs, T/L	6.47±0.46	6.34±0.51	6.34±0.51	6.51±0.48
MCV, fL	91.6±6.0	97.8±11.9	99.7±12.2	100.8±8.3**
SD-RDW, fL	48.2±1.8	54.0±7.7	55.6±8.5	58.8±13.3
Glucose, mg/dL	481.4±33.0	254.0±31.5**	211.1±34.4**	174.1±37.1**
Lactate, mM	6.57±0.96	32.66±3.42**	37.24±3.64**	35.95±3.87**
MVs, 1/µL	3,628±1,047	7,980±832++*	15,860±4,219**	258,654±106,413*
% haemolysis	0.079±0.017	0.233±0.062*	0.441±0.135**	3.817±1.391**
AOP, nW	71.4±5.3	62.3±9.2++	61.4±5.6*	62.2±6.5
GSH, µmol/g Hb	5.27±0.42+	5.46±0.62	4.08±0.33*	2.21±0.38**
GSSG, nmol/g Hb	28.2±5.2	35.0±4.9*	27.3±4.4	178.0±118.7
SD-OPD, nm	49.6±6	46.6±2.2*	55.5±6	86.8±8.9**
% stomatocytes	30.0±14.4	18.0±4.2	13.7±3.7	6.7±2.7
% discocytes	64.0±13.6	69.7±4.8	60.0±7.0	20.8±8.4*
% echinocytes	5.8±1.8	10.8±7.0	15.7±7.0	14.2±5.7
% spherocytes	0.1±0.1	1.5±0.8*	10.6±5.9*	58.3±13.0**
CMF discocytes, nm	30.4±3.5+	29.5±2.9	29.9±3.1	29.0±2.9
CMF spherocytes, nm	32.1±4.1+	27.5±3.2	28.1±3.4	27.9±3.4

Mean values of 5 ECs ± standard deviation. Measures taken at day 4+ instead of day 1 or day 31++ instead of day 29.
*p<0.05, **p<0.01 compared to day 1. RBC: red blood cells; MCV: mean RBC corpuscular volume; SD-RDW: RBC distribution width; MVs: microvesicles; AOP: antioxidant power; GSH: intracellular reduced glutathione; GSSG: intracellular oxidised glutathione; SD-OPD: standard deviation of the optical path difference distribution; CMF: cell membrane fluctuations.

Similarly to the AOP, intracellular concentration of GSH increased during the first two weeks of storage from 5.27±0.42 µmol/g Hb at day 4 to 6.35±0.39 µmol/g Hb at day 15 (Figure 1C, right). It then dropped to 4.08±0.33 µmol/g Hb after 43 days and 2.21±0.38 µmol/g Hb after day 71 of storage. In the 5 ECs, GSSG levels remained low until day 43 (28.2±5.2 nmol/g Hb at day 1, 27.3±4.4 at day 43) and increased drastically up to 178.0±118.7 nmol/g Hb at day 71 (refer to Online Supplementary Content). These values were quite variable among donors. These results correlate with the increased metabolic activity observed by our group and others between 7 and 14 days of storage, followed by its decrease due to lactate-associated drop of pH[3,67]. As glycolysis is progressively inhibited by low temperature and pH, glucose is consumed *via* the PPP, producing NADPH. This metabolite is the co-factor of the glutathione reductase responsible for the recycling of GSSG into GSH, a major thiol-based antioxidant in RBCs. However, the PPP does not produce enough NADPH to sustain recycling of glutathione all along the storage. Additionally, glutathione *de novo* synthesis is ATP-dependent and is therefore impaired when the stocks of intracellular ATP are depleted.

The loss of metabolites and antioxidants defenses correlates with the accumulation of oxidised biomolecules and the apparition of irreversible lesions[20-22,27,68].

Microvesicles and haemolysis

Microvesiculation and haemolysis followed the same trend. The number of MVs in the ECs increased first linearly from day 1 (3,628±1,047 MVs/µL) to day 36 (8,591±971 MVs/µL, 2.4-fold increase), before increasing exponentially between day 43 (15,860±4,219 MVs/µL, 4.4-fold increase) and day 71 (258,654±106,413 MVs/µL, 71.3-fold increase) (Figure 1D, left). Similarly, mean haemolysis percentage (0.079±0.017% at day 1) (Figure 1D, right) increased linearly until day 36 (0.28±0.06%, 3.5-fold increase), before raising exponentially. Mean haemolysis was of 0.44±0.14% (5.6-fold increase) at day 43, and of 3.82±1.39% (48.3-fold increase) after 71 days of storage. The exponential release of MVs as well as the haemolysis, are probably reflecting the accumulation of waste products inside the cell and apparition of

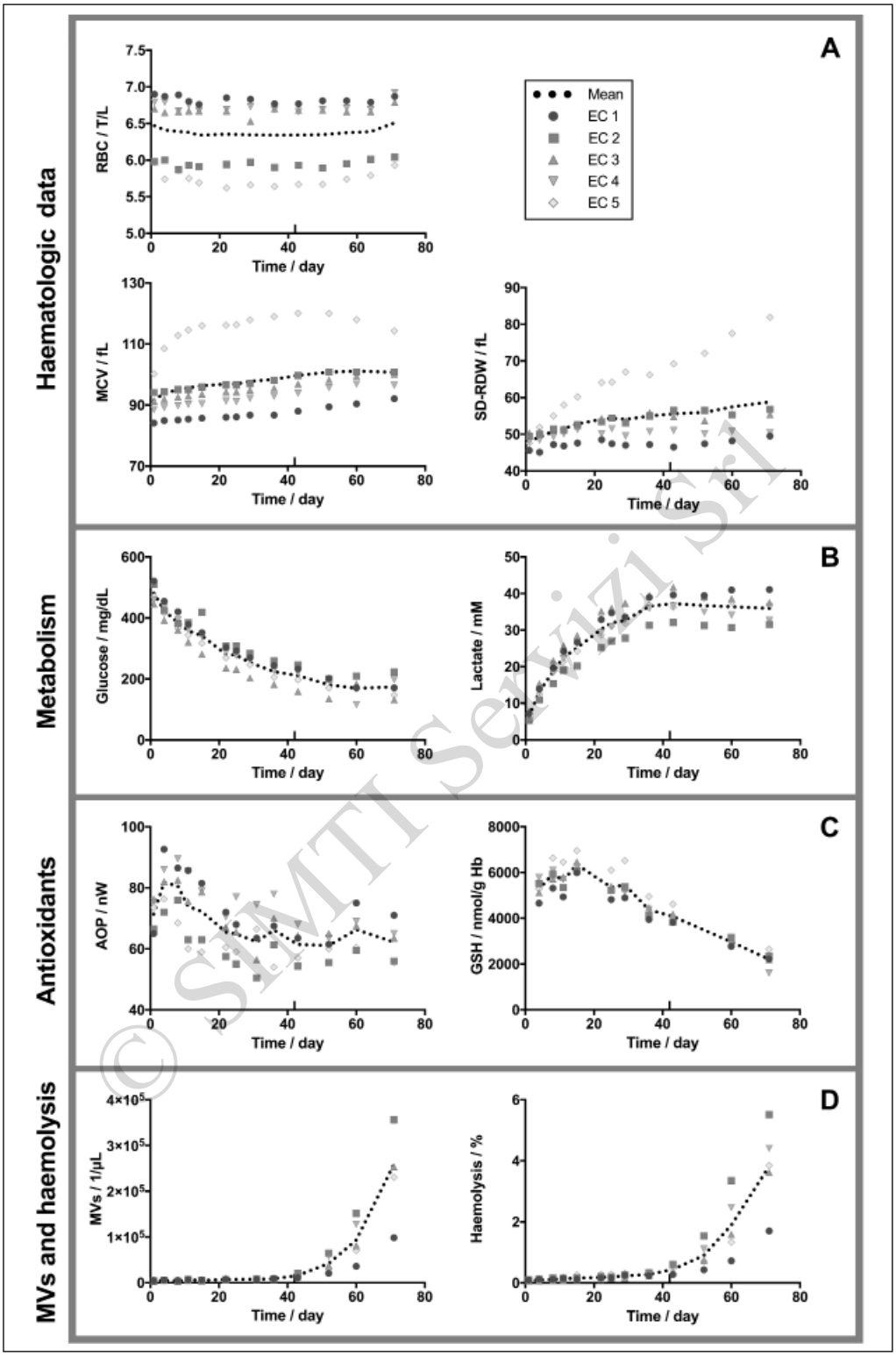

Figure 1 - Red blood cells (RBC) aging markers for erythrocyte concentrates (ECs) 1-5 stored during 71 days.
(A) Haematologic data (RBC count, mean RBC corpuscular volume [MCV] and RBC distribution width [SD-RDW]); (B) metabolic (glucose and lactate concentrations); (C) antioxidant (global antioxidant power [AOP] and intracellular reduced glutathione [GSH] concentration); (D) microvesicles (MVs) and haemolysis; data for ECs 1-5 stored during 71 days.
Individual (symbols) and mean values (dotted line) are presented ± standard deviation.

irreversible lesions at the level of the cytoskeleton and plasma leading together to the destabilisation of the RBC membrane (it is to be mentioned that cell debris coming from haemolysed RBCs could be wrongly detected as MVs by the flow cytometer). Again, it is interesting to notice that the measured values were quite different among the 5 ECs.

Morphology analysis with digital holographic microscopy

Population and single-cell analysis of red blood cell morphology

All ECs at the exception of EC 5 had a similar SD-OPD at the beginning of the storage. The baseline mean SD-OPD was 49.6±6.0 nm at day 1. SD-OPD value remained stable until day 29, and then increased to reach 55.5±6.0 nm at day 43 and 86.8±8.9 nm at day 71 (Figure 2A, left). Increasing SD-OPD value was strongly correlated to the transformation of discocytes into transient echinocytes and finally spherocytes in the ECs (refer to Online Supplementary Content). At day 1, RBCs were mostly discocytes (64.0±13.6%) or stomatocytes (30.0±14.4%) (Figure 2A, right). Until day 29, stomatocytes transformed into discocytes, together these two cell types represented approximately 95% of the population. Population of discocytes started to drop linearly from day 36. After 29 days, spherocytes that represented less than 1% of the population at the beginning of storage started to appear in ECs. From this point, the percentage of spherocytes also increased linearly in the sample to reach 10.6±5.9% at day 43 and 58.3±13.0% at day 71. Echinocytes are a transitional intermediate between discocytes and spherocytes, explaining why their number did not increase. Morphological changes followed biochemical alterations, thus suggesting causative events. EC 5 morphology differed widely (refer to Online Supplementary Content), whereas it was not the case for other parameters like the MV count or haemolysis level. Discrepancies in RBC "storability" could be linked to the donors' characteristics such as its age (EC 5 was the youngest donor), lifestyle or genetic background[69-71].

Membrane fluctuations

Morphological classes of RBCs can be distinguished based on their CFM map (Figure 2B). For instance,

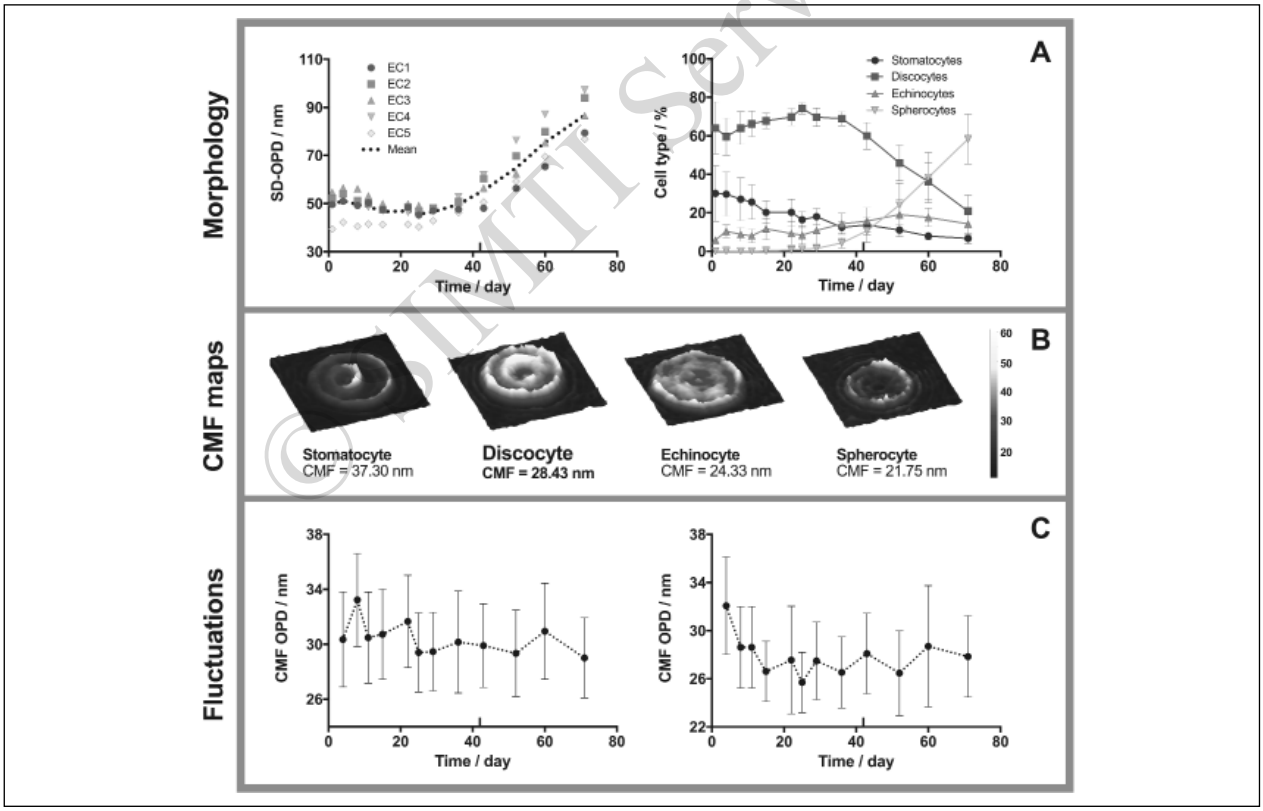

Figure 2 - DHM analysis of red blood cells (RBC) for erythrocyte concentrates (ECs) 1-5 stored during 71 days. (A) Morphology of RBC population (standard deviation of the optical path difference distribution, SD-OPD) and single-cell (CellProfiler and CellProfiler Analyst); (B) cell membrane fluctuations (CMF) map for different classes of RBCs, and (C) CMF changes for discocytes (left) and spherocytes (right). Twelve images (3 wells per EC and 4 images per well) and 3 movies (1 per well) were acquired for each EC. Mean values are presented ± standard deviation.

discocytes present a symmetric fluctuation in their center and their ring while echinocytes have a decreased center fluctuation. Interestingly, when RBCs become spherocytes, fluctuations in the central area are no longer observed. In stomatocytes there is an asymmetric fluctuation in membrane surface related to the asymmetrical shape of the RBC. The CMF values can be ranked in the following order (by decreasing order of CMF amplitude): stomatocyte, discocyte, echinocyte, spherocyte. As expected the spherocytes exhibited the lower CMF values which corroborates their loss of flexibility[72]. Stomatocytes that have a loose part enable an important fluctuation in this region. Finally, the functional state (i.e. discocytes) exhibits the highest CMF.

A general analysis shows a constant decrease of the CMF during the storage. CMF of discocytes is decreasing while RBCs are getting older (Figure 2C, left). They lost 10% of their CMF at the expiration date. Regarding spherocytes, after a decrease phase, a plateau was reached at day 18 (Figure 2C, right). The decrease of CMF is interesting as it is measured on a changing population (discocytes that change their shape to spherocyte are no longer included in the discocyte CMF analysis), thus suggesting that not only the shape of the RBCs is responsible for the decreasing CFM but that other aspects such as cell metabolism and membrane integrity are also involved in this physiological change.

One of the important result from the CMF fluctuations analysis is that even when RBCs keep an intact discocyte shape, their fluctuations amplitude decreases, suggesting that aging not only induces morphological changes from discocytes to spherocytes, but also alter the state of the RBCs that keep their discocyte shape. During the first 3 weeks of storage and following the main metabolism lesions, RBCs lost a part of their fluctuations capacity. Several mechanisms could participate to it such as phosphorylation events that are dependent of energy metabolism[73].

Conclusions

RBCs accumulate a broad range of lesions during storage under standard blood transfusion practice. Of particular interest is the sequence of events that leads to the storage lesions with 2 cornerstones and 3 zones[68]. Some of these lesions are irreversible once transfused in the patient. Extensively damaged RBCs are rapidly cleared from the circulation of the transfusion recipient, therefore decreasing the beneficial impact of the treatment[42]. Worse, the accumulation of free iron and Hb as well as MVs could lead to adverse transfusion reactions[45,49,50]. It raises questions concerning transfusion practices related to the age of ECs and are in agreement with the retrospective clinical study of Goel *et al.* showing that the risks (morbidity, mortality or length of stay in hospital) associated to the transfusion of ECs older than 28 or 35 days are higher compared to those 21 days or younger[9].

As already stated, important differences appeared when looking at ECs ageing markers individually[71,74]. For example, it was demonstrated that RBCs from donors exhibiting high levels of plasma uric acid antioxidant aged better than those having low-levels of uric acid[66]. Inter-donor variability is linked to sex, age, ethnic groups, blood group, weight, genetic background and lifestyle[75]. Biomarkers offer unique tools to assess RBC health state. AOP can be an easy-to-monitor single parameter allowing a quick glance at the cell state. Furthermore, combining multiple easy-to-obtain parameters providing different information like AOP (yielding information on oxidative stress), percentage of spherocytes (yielding information about morphological perturbation), and CMF (yielding information on membrane state) could greatly help quantify RBC ageing and help discard prematurely old RBC pouches before transfusion.

Acknowledgements

The Authors thank Dr Philippe Tacchini who provided the Edelmeter instrument and chips.

Funding

The Authors thank the research committee of "Transfusion SRC Switzerland" and the CETRASA foundation for the grant entitled "New routes and new additive solution formulations to improve the quality of stored red blood cells" for financial support. This research was also supported in part by the Basic Science Research Program through the National Research Foundation of Korea (NRF) funded by the Ministry of Science, ICT & Future Planning (NRF-2015K1A1A2029224).

Authorship contributions

MB, BR and MP conducted the project and wrote the manuscript. MB prepared and analysed the RBCs. DC quantified the microvesicles in the samples. BR and MB did the DHM experiments. KJ and IM carried out the CMF analyses. J-DT, GT and NL reviewed data and manuscript. All the Authors read and approved the final version of the manuscript.

Disclosure of conflicts of interest

BR also works part-time for Lyncée Tec which commercialises the DHM used in this study. The other Authors declare no conflicts of interest.

References

1) Hess JR. Red cell changes during storage. Transfus Apher Sci 2010; **43**: 51-9.
2) Lion N, Crettaz D, Rubin O, Tissot J-D. Stored red blood

cells: A changing universe waiting for its map(s). J Proteomics 2010; **73**: 374-85.
3) D'Alessandro A, D'Amici GM, Vaglio S, Zolla L. Time-course investigation of SAGM-stored leukocyte-filtered red bood cell concentrates: from metabolism to proteomics. Haematologica 2012; **97**: 107-15.
4) Flatt JF, Bawazir WM, Bruce LJ. The involvement of cation leaks in the storage lesion of red blood cells. Front Physiol 2014; **5**: 214.
5) Prudent M, Tissot JD, Lion N. The three-phase evolution of stored red blood cells and the clinical trials: an obvious relationship. Blood Transfus 2017; **15**: 188.
6) Koch CG, Li L, Sessler DI, et al. Duration of red-cell storage and complications after cardiac surgery. Engl J Med 2008; **358**: 1229-39.
7) Spinella PC, Carroll CL, Staff I, et al. Duration of red blood cell storage is associated with increased incidence of deep vein thrombosis and in hospital mortality in patients with traumatic injuries. Crit Care Lond Engl 2009; **13**: R151.
8) Solomon SB, Wang D, Sun J, et al. Mortality increases after massive exchange transfusion with older stored blood in canines with experimental pneumonia. Blood 2013; **121**: 1663-72.
9) Goel R, Johnson DJ, Scott AV, et al. Red blood cells stored 35 days or more are associated with adverse outcomes in high-risk patients. Transfusion 2016; **56**: 1690-8.
10) Lacroix J, Hébert PC, Fergusson DA, et al. Age of transfused blood in critically ill adults. N Engl J Med 2015; **372**: 1410-8.
11) Steiner ME, Ness PM, Assmann SF, et al. Effects of red-cell storage duration on patients undergoing cardiac surgery. N Engl J Med 2015; **372**: 1419-29.
12) Heddle NM, Cook RJ, Arnold DM, et al. Effect of short-term vs. long-term blood storage on mortality after transfusion. N Engl J Med 2016; **375**: 1937-194.
13) Klein H, Cortés-Puch I, Natanson C. More on the age of transfused red cells. N Engl J Med 2015; **373**: 283.
14) Scott KL, Lecak J, Acker JP. Biopreservation of Red blood cells: past, present, and future. Transfus Med Rev 2005; **19**: 127-42.
15) D'Alessandro A, Kriebardis AG, Rinalducci S, et al. An update on red blood cell storage lesions, as gleaned through biochemistry and omics technologies. Transfusion 2015; **55**: 205-19.
16) Hess JR, Rugg N, Joines AD, et al. Buffering and dilution in red blood cell storage. Transfusion 2006; **46**: 50-4.
17) Veale MF, Healey G, Sran A, et al. AS-7 improved in vitro quality of red blood cells prepared from whole blood held overnight at room temperature. Transfusion 2015; **55**: 108-14.
18) Bennett-Guerrero E, Veldman TH, Doctor A, et al. Evolution of adverse changes in stored RBCs. Proc Natl Acad Sci 2007; **104**: 17063-8.
19) Paglia G, D'Alessandro A, Rolfsson Ó, et al. Biomarkers defining the metabolic age of red blood cells during cold storage. Blood 2016; **28**: e43-50.
20) Delobel J, Prudent M, Tissot J-D, Lion N. Proteomics of the red blood cell carbonylome during blood banking of erythrocyte concentrates. Proteomics Clin Appl 2016; **10**: 257-66.
21) Delobel J, Prudent M, Rubin O, et al. Subcellular fractionation of stored red blood cells reveals a compartment-based protein carbonylation evolution. J Proteomics 2012; **76**: 181-93.
22) Kriebardis AG, Antonelou MH, Stamoulis KE, et al. Progressive oxidation of cytoskeletal proteins and accumulation of denatured hemoglobin in stored red cells. J Cell Mol Med 2007; **11**: 148-55.
23) Pallotta V, Rinalducci S, Zolla L. Red blood cell storage affects the stability of cytosolic native protein complexes. Transfusion 2015; **55**: 1927-36.
24) Rinalducci S, Marrocco C, Zolla L. Thiol-based regulation of glyceraldehyde-3-phosphate dehydrogenase in blood bank-stored red blood cells: a strategy to counteract oxidative stress. Transfusion 2015; **55**: 499-506.
25) Sparrow RL, Sran A, Healey G, et al. In vitro measures of membrane changes reveal differences between red blood cells stored in saline-adenine-glucose-mannitol and AS-1 additive solutions: a paired study: SAGM and AS-1 RBCs. Transfusion 2014; **54**: 560-8.
26) Antonelou MH, Kriebardis AG, Stamoulis KE, et al. Red blood cell aging markers during storage in citrate-phosphate-dextrose-saline-adenine-glucose-mannitol. Transfusion 2010; **50**: 376-89.
27) Kriebardis AG, Antonelou MH, Stamoulis KE, et al. Membrane protein carbonylation in non-leukodepleted CPDA-preserved red blood cells. Blood Cells Mol Dis 2006; **36**: 279-82.
28) Kriebardis AG, Antonelou MH, Stamoulis KE, et al. RBC-derived vesicles during storage: ultrastructure, protein composition, oxidation, and signaling components. Transfusion 2008; **48**: 1943-53.
29) Zolla L, D'Alessandro A, Rinalducci S, et al. Classic and alternative red blood cell storage strategies: seven years of "-omics" investigations. Blood Transfus 2015; **13**: 21-31.
30) Reisz JA, Wither MJ, Dzieciatkowska M, et al. Oxidative modifications of glyceraldehyde 3-phosphate dehydrogenase regulate metabolic reprogramming of stored red blood cells. Blood 2016; **128**: e32-e42.
31) Rinalducci S, D'Amici GM, Blasi B, et al. Peroxiredoxin-2 as a candidate biomarker to test oxidative stress levels of stored red blood cells under blood bank conditions: Prx2 as oxidative stress marker in stored RBCs. Transfusion 2011; **51**: 1439-49.
32) Wither M, Dzieciatkowska M, Nemkov T, et al. Hemoglobin oxidation at functional amino acid residues during routine storage of red blood cells: Hb oxidation in stored RBCs and vesicles. Transfusion 2016; **56**: 421-6.
33) Rubin O, Crettaz D, Canellini G, et al. Microparticles in stored red blood cells: an approach using flow cytometry and proteomic tools. Vox Sang 2008; **95**: 288-97.
34) Gao Y, Lv L, Liu S, et al. Elevated levels of thrombin-generating microparticles in stored red blood cells. Vox Sang 2013; **105**: 11-7.
35) Jy W, Johansen ME, Bidot C, et al. Red cell-derived microparticles (RMP) as haemostatic agent. Thromb Haemost 2013; **11**: 751-60.
36) Berezina TL, Zaets SB, Morgan C, et al. Influence of storage on red blood cell rheological properties. J Surg Res 2002; **102**: 6-12.
37) Blasi B, D'Alessandro A, Ramundo N, Zolla L. Red blood cell storage and cell morphology. Transfus Med 2012; **22**: 90-6.
38) Mohandas N, Evans E. Mechanical properties of the red cell membrane in relation to molecular structure and genetic defects. Annu Rev Biophys Biomol Struct 1994; **23**: 787-818.
39) Diez-Silva M, Dao M, Han J, et al. Shape and biomechanical characteristics of human red blood cells in health and disease. MRS Bull 2010; **35**: 382-8.
40) Park Y, Best CA, Auth T, et al. Metabolic remodeling of the human red blood cell membrane. Proc Natl Acad Sci 2010; **107**: 1289-94.
41) Duez J, Holleran JP, Ndour PA, et al. Mechanical clearance of red blood cells by the human spleen: Potential therapeutic applications of a biomimetic RBC filtration method. Transfus Clin Biol 2015; **22**: 151-7.
42) Safeukui I, Buffet PA, Deplaine G, et al. Quantitative assessment of sensing and sequestration of spherocytic erythrocytes by the human spleen. Blood 2012; **120**: 424-30.
43) Sowemimo-Coker SO. Red blood cell hemolysis during processing. Transfus Med Rev 2002; **16**: 46-60.
44) D'Alessandro A, Dzieciatkowska M, Hill RC, Hansen KC. Supernatant protein biomarkers of red blood cell storage hemolysis as determined through an absolute quantification proteomics technology. Transfusion 2016; **56**: 1329-39.

45) Hod EA, Brittenham GM, Billote GB, et al. Transfusion of human volunteers with older, stored red blood cells produces extravascular hemolysis and circulating non-transferrin-bound iron. Blood 2011; **118**: 6675-82.
46) Luten M, Roerdinkholder-Stoelwinder B, Schaap NPM, et al. Survival of red blood cells after transfusion: a comparison between red cells concentrates of different storage periods. Transfusion 2008; **48**: 1478-85.
47) Baek JH, D'Agnillo F, Vallelian F, et al. Hemoglobin-driven pathophysiology is an in vivo consequence of the red blood cell storage lesion that can be attenuated in guinea pigs by haptoglobin therapy. J Clin Invest 2012; **122**: 1444-58.
48) Schaer DJ, Buehler PW, Alayash AI, et al. Hemolysis and free hemoglobin revisited: exploring hemoglobin and hemin scavengers as a novel class of therapeutic proteins. Blood 2013; **121**: 1276-84.
49) Hod EA, Spitalnik SL. Stored red blood cell transfusions: Iron, inflammation, immunity, and infection. Transfus Clin Biol 2012; **19**: 84-9.
50) Hod EA, Zhang N, Sokol SA, et al. Transfusion of red blood cells after prolonged storage produces harmful effects that are mediated by iron and inflammation. Blood 2010; **115**: 4284-92.
51) Tacchini P, Lesch A, Neequaye A, et al. Electrochemical pseudo-titration of water-soluble antioxidants. Electroanalysis 2013; **25**: 922-30.
52) Prudent M, Muller M, Maye S, et al. The antioxidant defense system of erythrocyte concentrates is increased during the first week of storage. Transfusion 2016; **56**: 56A-7A.
53) Boss D, Hoffmann A, Rappaz B, et al. Spatially-resolved eigenmode decomposition of red blood cells membrane fluctuations questions the role of ATP in flickering. PLoS ONE 2012; **7**: e40667.
54) Giustarini D, Dalle-Donne I, Milzani A, et al. Analysis of GSH and GSSG after derivatization with N-ethylmaleimide. Nat Protoc 2013; **8**: 1660-9.
55) Han V, Serrano K, Devine DV. A comparative study of common techniques used to measure haemolysis in stored red cell concentrates. Vox Sang 2010; **98**: 116-23.
56) Prudent M, Stauber F, Rapin A, et al. Small-scale perfusion bioreactor of red blood cells for dynamic studies of cellular pathways: proof-of-concept. Front Mol Biosci 2016; **3**: 11.
57) Marquet P, Rappaz B, Magistretti PJ, et al. Digital holographic microscopy: a noninvasive contrast imaging technique allowing quantitative visualization of living cells with subwavelength axial accuracy. Opt Lett 2005; **30**: 468.
58) Rappaz B, Breton B, Shaffer E, Turcatti G. Digital Holographic Microscopy: a quantitative label-free microscopy technique for phenotypic screening. Comb Chem High Throughput Screen 2014; **14**: 80.
59) Kühn J, Shaffer E, Mena J, et al. Label-free cytotoxicity screening assay by digital holographic microscopy. Assay Drug Dev Technol 2013; **11**: 101-7.
60) Rappaz B, Barbul A, Emery Y, et al. Comparative study of human erythrocytes by digital holographic microscopy, confocal microscopy, and impedance volume analyzer. Cytometry A 2008; **73A**: 895903.
61) Rappaz B, Marquet P, Cuche E, et al. Measurement of the integral refractive index and dynamic cell morphometry of living cells with digital holographic microscopy. Opt Express 2005; **13**: 9361-73.
62) Carpenter AE, Jones TR, Lamprecht MR, et al. CellProfiler: image analysis software for identifying and quantifying cell phenotypes. Genome Biol 2006; **7**: R100.
63) Thevenaz P, Ruttimann UE, Unser M. A pyramid approach to subpixel registration based on intensity. IEEE Trans. Image Process 1998; **7**: 27-41.
64) Schneider CA, Rasband WS, Eliceiri KW. NIH image to ImageJ: 25 years of image analysis. Nat Methods 2012; **9**: 671-5.
65) Rappaz B, Barbul A, Hoffmann A, et al. Spatial analysis of erythrocyte membrane fluctuations by digital holographic microscopy. Blood Cells Mol Dis 2009; **42**: 228-32.
66) Tzounakas VL, Georgatzakou HT, Kriebardis AG, et al. Uric acid variation among regular blood donors is indicative of red blood cell susceptibility to storage lesion markers: A new hypothesis tested. Transfusion 2015; **55**: 2659-71.
67) Bordbar A, Johansson PI, Paglia G, et al. Identified metabolic signature for assessing red blood cell unit quality is associated with endothelial damage markers and clinical outcomes. Transfusion 2016; **56**: 852-62.
68) Prudent M, Tissot J-D, Lion N. In vitro assays and clinical trials in red blood cell aging: Lost in translation. Transfus Apher Sci 2015; **52**: 270-6.
69) Kanias T, Lanteri MC, Keating S, et al. Effect of age, sex or frequent blood donations on donors' ferritin levels and red blood cell storage stability. Transfusion 2016; **56**: 3A-262A.
70) Antonelou MH, Seghatchian J. Insights into red blood cell storage lesion: toward a new appreciation. Transfus Apher Sci 2016; **55**: 292-301.
71) Tzounakas VL, Georgatzakou HT, Kriebardis AG, et al. Donor variation effect on red blood cell storage lesion: a multivariable, yet consistent, story. Transfusion 2016; **56**: 1274-86.
72) Evans J, Gratzer W, Mohandas N, et al. Fluctuations of the red blood cell membrane: relation to mechanical properties and lack of ATP dependence. Biophys J 2008; **94**: 4134-44.
73) Prudent M, Rappaz B, Hamelin R, et al. Loss of protein tyrphosphorylation during in vitro storage of human erythrocytes: impact on RBC morphology. Transfusion 2014; **54**: 49A-50A.
74) Dern RJ, Gwinn RP, Wiorkowski JJ. Studies on the preservation of human blood. I. Variability in erythrocyte storage characteristics among healthy donors. J Lab Clin Med 1966; **67**: 955-65.
75) Tzounakas VL, Kriebardis AG, Papassideri IS, Antonelou MH. Donor-variation effect on red blood cell storage lesion: A close relationship emerges. Proteomics Clin Appl 2016; **10**: 791-804.

Arrived: 14 November 2016 - Revision accepted: 5 December 2016
Correspondence: Michel Prudent
Transfusion Interrégionale CRS
Laboratoire de Recherche sur les Produits Sanguins
Route de la Corniche 2
1066 Epalinges, Switzerland
e-mail: michel.prudent@itransfusion.ch